

Lawrence Berkeley National Laboratory

Lawrence Berkeley National Laboratory

Title

MASS TRANSFER TO ROTATING DISKS AND ROTATING RINGS IN LAMINAR, TRANSITION, AND FULLY DEVELOPED TURBULENT FLOW

Permalink

<https://escholarship.org/uc/item/4hs762jt>

Author

Law Jr., C.G.

Publication Date

1980-07-01

c.2



Lawrence Berkeley Laboratory

UNIVERSITY OF CALIFORNIA

Materials & Molecular Research Division

Submitted to the International Journal of Heat and
Mass Transfer

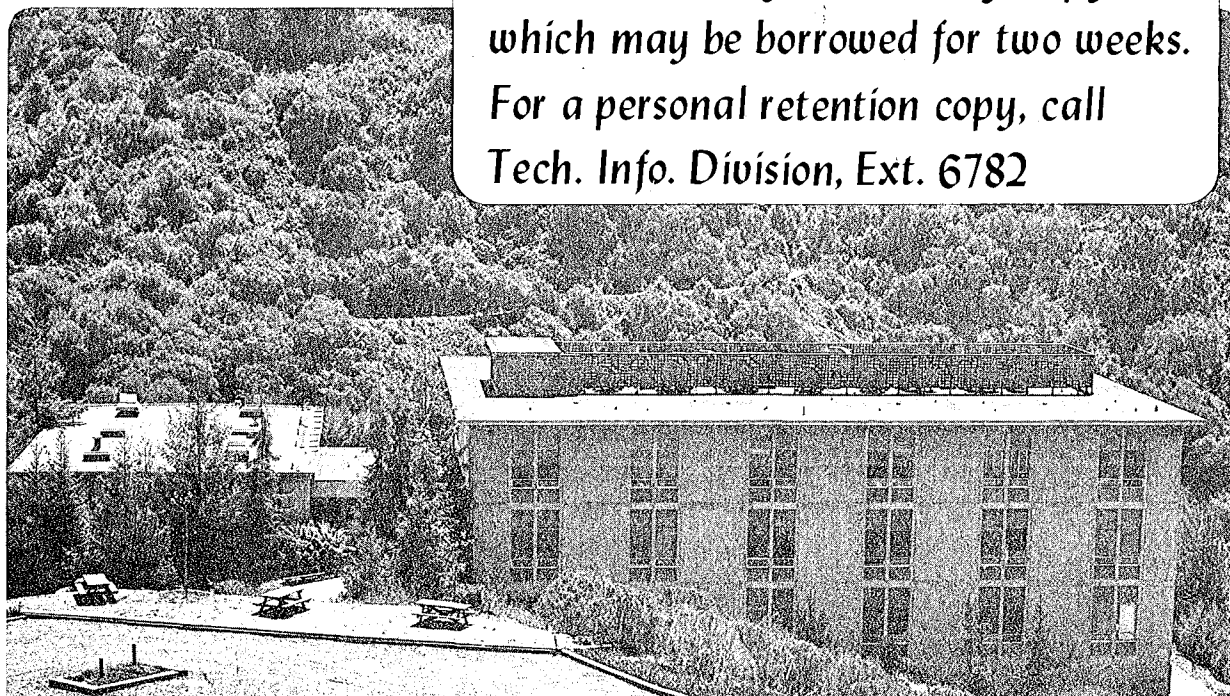
MASS TRANSFER TO ROTATING DISKS AND ROTATING RINGS IN
LAMINAR, TRANSITION, AND FULLY DEVELOPED TURBULENT FLOW

Clarence G. Law, Jr., Peter Pierini, and John Newman

July 1980

TWO-WEEK LOAN COPY

*This is a Library Circulating Copy
which may be borrowed for two weeks.
For a personal retention copy, call
Tech. Info. Division, Ext. 6782*



LBL-11241
c.2

Mass Transfer to Rotating Disks and Rotating Rings in
Laminar, Transition, and Fully Developed Turbulent Flow

Clarence G. Law, Jr., Peter Pierini, and John Newman

Materials and Molecular Research Division, Lawrence Berkeley Laboratory
and Department of Chemical Engineering, University of California,
Berkeley, California 94720

July 1980

Abstract

Experimental data and theoretical calculations are presented for the mass-transfer rate to rotating disks and rotating rings when laminar, transition, and fully developed turbulent flow exist upon different portions of the surface. Good agreement of data and the model is obtained for rotating disks and relatively thick rotating rings. Results of the calculations for thin rings generally exceed the experimental data measured in transition and turbulent flow. A $y^+{}^3$ form for the eddy diffusivity is used to fit the data. No improvement is noticed with a form involving both $y^+{}^3$ and $y^+{}^4$.

Introduction

On rotating disks and rotating rings, the flow regime may vary from laminar near the center to fully developed turbulent flow near the periphery. The fundamentals of fluid flow and mass transfer are well characterized in laminar flow. However, transition flow, existing between laminar and fully developed turbulent flow, along with the developed turbulent flow regime have not been described to the same extent. Correlations of experimental results form the basis of most of the available information concerning the mass-transfer rates for these systems.

Mohr and Newman [1] provide experimental results for the Sherwood number in the laminar, transition, and fully developed turbulent regions of a rotating disk. In addition, they considered the transition region to exist for Reynolds numbers from 2×10^5 to 3×10^5 . This range is similar to values reported by Gregory, Stuart, and Walker [2], Cobb and Saunders [3], Kreith, Taylor, and Chong [4], Tien and Campbell [5], Ellison and Coronet [6], and Chin and Litt [7]. For the transition region Mohr and Newman give

$$\bar{Sh} = (9.7 \times 10^{-15} Re^3 + 0.89 \times 10^5 Re^{-1/2}) Sc^{1/3} \quad (1)$$

and for fully developed turbulent flow

$$\bar{Sh} = (0.0078 Re^{0.9} - 1.30 \times 10^5 Re^{-1/2}) Sc^{1/3} \quad (2)$$

where the Sherwood number is defined for disks or rings as

$$\bar{Sh} = \frac{\bar{ir}_o}{nFDC_\infty} = \frac{\int_{r_i}^{r_o} 2\pi r i(r) dr}{\pi(r_o^2 - r_i^2) nFDC_\infty} \quad (3)$$

Additional studies of mass transfer to a rotating disk have been reported by Ellison and Coronet as

$$\overline{Sh} = 0.0117 Re^{0.896} Sc^{0.249} \quad \text{for } Re > 10^6 \quad (4)$$

and also be Daguinet [8] as

$$\overline{Sh} = 0.00725 Re^{0.9} Sc^{0.33} \quad \text{for } Re > 10^5 . \quad (5)$$

The different Schmidt and Reynolds number dependences are indicative of the scatter in the data. Modification of the multiplicative constant and the two exponents makes it possible to represent the data, due to scatter, with slightly different expressions. Because of the scatter in the data, it is also difficult to distinguish between a 1/3 and 1/4 power Schmidt number dependence.

Average mass-transfer rates are measured and hence average-Sherwood-number correlations are obtained directly. The data must be differentiated to obtain information on local mass-transfer rates. Differentiation of data with considerable scatter may not give reliable information. To model accurately mass-transfer processes on a rotating disk (as in corrosion), reliable local mass-transfer rates are required. Therefore, the approach taken here is to develop a model from which local mass-transfer rates can be calculated. These local rates can then be integrated for comparison with measured average mass-transfer rates. This general approach was used by Kader and Dil'man [9] in pipe flow.

In the study of corrosion on a rotating disk, local mass-transfer rates are needed when the mass transfer commences at an arbitrary radial

position on the surface. This is analagous to rotating rings with different thicknesses. Daguinet [8] and Delouis and Keddam [10] have investigated mass-transfer rates on ring electrodes of various dimensions in the transition and turbulent regimes. Data taken by Delouis and Keddam on thick rings support a 0.9 exponent on the Reynolds number, similar to disk correlations. However, for thin rings the data gave rise to an exponent of 0.6. These authors also reported measured values of the limiting current for thin rings in transition and turbulent flow which lie below the Levich [11] relationship for thin rings. This deviation in limiting currents cannot be explained in terms of radial diffusion. Newman [12,13] has considered the importance of radial diffusion to a flat plate and to a rotating disk at the limiting current. Radial diffusion is important in a very small region and its effect is to increase the mass-transfer rate.

From an analytic viewpoint, few models exist which describe the mass transfer to rotating disks and rotating rings beyond the laminar flow region. Chin and Litt [7] express the Sherwood number for thin rings in terms of the shear stress. Cognet and Daguinet [14] along with Kornienko and Kishinevskii [15] have presented models for disks and rings in turbulent flow. In the work by Kornienko and Kishinevskii the problem was solved for developed and undeveloped diffusion boundary layers. They also state that it is not possible to distinguish between the $1/3$ and $1/4$ Schmidt number dependence from rotating-ring data due to the different levels of development of the diffusion boundary layer.

An approach to solving heat and mass-transfer problems in turbulent flow without á priori solution of the Navier-Stokes equations was presented by Spalding [16] some time ago. Spalding's results are for a Prandtl

number of one. This work has been the subject of further investigation, review, and extension by Kestin and Presen [17], Kestin and Richardson [18], and Donovan, Hanna, and Yerazunis [19]. Numerical results have been presented by Smith and Shah [20] for low Prandtl numbers and extensive tabulations were presented by Gardner and Kestin [21] for Prandl numbers up to 1000. Although the model developed herein is based on solving the time averaged convective-diffusion equation in terms of the Lighthill [22] variable, we would be remiss not to mention the applicability of Spalding's transformation for two-dimensional and axisymmetric problems with high Schmidt numbers. However, both approaches are comparable in that the shear stress is required in addition to a form for turbulent transfer near the wall, but solution of the Navier-Stokes equations is not required.

Model Development

The boundary-layer form of the time-averaged convective-diffusion equation is the governing equation for mass transfer.

$$v_r \frac{\partial \theta}{\partial r} + v_y \frac{\partial \theta}{\partial y} = \frac{\partial}{\partial y} \left[(D+D^{(t)}) \frac{\partial \theta}{\partial y} \right] \quad (6)$$

$$\theta \rightarrow 1 \quad \text{as } y \rightarrow \infty$$

$$\theta = 0 \quad \text{at } y = 0, \quad r \geq r_i$$

$$\theta = 1 \quad \text{at } y = 0, \quad r < r_i.$$

v_r can be expressed as

$$v_r = \beta(r)y, \quad (7)$$

and v_y is given by the equation of continuity as

$$v_y = -\frac{1}{2} y^2 \frac{(r\beta)'}{r} \quad (8)$$

With the Lighthill variable

$$\xi = \frac{y\sqrt{r\beta}}{\left[9D \int_{r_i}^r r \sqrt{r\beta} dr \right]^{1/3}}, \quad (9)$$

equation (6) can be expressed as

$$\frac{\xi}{r\sqrt{r\beta}} \left[9 \int_{r_i}^r r \sqrt{r\beta} dr \right] \frac{\partial \theta}{\partial r} = 3\xi^2 \frac{\partial \theta}{\partial \xi} + \frac{\partial}{\partial \xi} \left[\left(1 + \frac{D^{(t)}}{D} \right) \frac{\partial \theta}{\partial \xi} \right] \quad (10)$$

At this point it is appropriate to comment on the form for $D^{(t)}/D$ or alternatively $D^{(t)}/\nu$. The concept of the universal velocity profile for fully developed turbulent flow suggests that $D^{(t)}/\nu$ depends only on a dimensionless distance y^+ from the wall in the form $y^+ = (y/\nu) \sqrt{\tau_o/\rho}$, where τ_o is the shear stress equal to $\mu\beta$.

Expansion of the velocity components in terms of y^+ shows that near the wall $D^{(t)}/\nu$ must be proportional to the cube of y^+ or a higher power of y^+ . With this in mind, many researchers [23-30] have expressed theoretical or experimental results in terms of

$$\frac{D^{(t)}}{\nu} = Ky^{+3} = K \left(\frac{y}{\nu} \sqrt{\frac{\tau_o}{\rho}} \right)^3, \quad (11)$$

whereas other investigators [16] [31-35] prefer

$$\frac{D^{(t)}}{\nu} = Ky^{+4} = K \left(\frac{y}{\nu} \sqrt{\frac{\tau_o}{\rho}} \right)^4 \quad (12)$$

Levich [36] initially advocated the $y^+{}^3$ form but subsequently [37] expressed a preference for equation (12). The form used in equation (10) will be kept sufficiently general so that a decision concerning the form of $D^{(t)}/\nu$ can be made in view of experimental and theoretical results. For this reason we let

$$\frac{D^{(t)}}{\nu} = Ky^+{}^3 d(y^+) \quad (13)$$

where $d(y^+)$ is a function of y^+ . For simplicity, $d(y^+)$ can be considered 1, and equation (11) is recovered. Substitution into equation (10) with the definitions

$$R = \sqrt{Re} = \sqrt{\frac{\Omega}{\nu}} r \quad (14)$$

$$X = \frac{9K}{\sqrt{\Omega}} \left(\frac{\Omega}{\nu}\right)^{5/4} \int_{r_i}^r r \sqrt{r\beta} dr = 9K \int_{R_i}^R R \sqrt{R \frac{\beta}{\Omega}} dR \quad (15)$$

$$\frac{\beta}{\Omega} = \frac{\tau_o}{\mu\Omega} \quad (16)$$

simplifies the governing equation and boundary conditions to

$$9X\xi \frac{\partial \theta}{\partial X} = 3\xi^2 \frac{\partial \theta}{\partial \xi} + \frac{\partial}{\partial \xi} \left[\left(1 + \frac{X\xi^3 d(X,\xi)}{R^{3/2}} \right) \frac{\partial \theta}{\partial \xi} \right] \quad (17)$$

$$\begin{aligned} \theta &= 1 & \xi &= \infty \\ \theta &= 0 & \xi &= 0 & X &\geq 0 \\ \theta &= 1 & \xi &= 0 & X &< 0 \end{aligned}$$

When $X = 0$, equation (17) simplifies to

$$\frac{d^2\theta}{d\xi^2} + 3\xi^2 \frac{d\theta}{d\xi} = 0 \quad (18)$$

This equation is analogous to the equation given by L  v  que [38], with the solution

$$\theta = \frac{1}{\Gamma(4/3)} \int_0^\xi e^{-y^3} dy . \quad (19)$$

For $X > 0$, equation (17) is solved using a Crank-Nicholson procedure.

The procedure is efficient and stable.

The local and average Sherwood numbers can be expressed as

$$Sh_{loc} = \frac{ir}{nFDC_\infty} = \frac{\partial\theta}{\partial\xi} \Big|_{\xi=0} R^{3/2} \sqrt{\frac{\beta}{\Omega}} \left(\frac{KSc}{X} \right)^{1/3} \quad (20)$$

$$\overline{Sh} = \frac{R_o \int_{R_i}^{R_o} \frac{\partial\theta}{\partial\xi} \Big|_{\xi=0} R^{3/2} \sqrt{\frac{\beta}{\Omega}} \left(\frac{KSc}{X} \right)^{1/3} dR}{(R_o^2 - R_i^2)} \quad (21)$$

The term $X\xi^3 d(X,\xi)/R^{3/2}$ in equation (17) accounts for the turbulent contribution to the mass-transfer rate. Equation (17) must be modified slightly to describe the three different transport mechanisms on the surface. A function $f(R)$ is introduced

$$9X\xi \frac{\partial\theta}{\partial X} = 3\xi^2 \frac{\partial\theta}{\partial\xi} + \frac{\partial}{\partial\xi} \left[\left(1 + \frac{X\xi^3 d(X,\xi)f(R)}{R^{3/2}} \right) \frac{\partial\theta}{\partial\xi} \right] \quad (22)$$

where $f(R)$ is defined as

$$f(R) = 0 \quad \text{Re} \leq 2.0 \times 10^5 \quad (23a)$$

$$f(R) = \frac{R - \sqrt{2 \times 10^5}}{\sqrt{3 \times 10^5} - \sqrt{2 \times 10^5}} \quad 2.0 \times 10^5 \leq \text{Re} \leq 3.0 \times 10^5 \quad (23b)$$

$$f(R) = 1 \quad \text{Re} \geq 3.0 \times 10^5 \quad (23c)$$

For laminar flow, the turbulent contribution to mass transfer disappears, since $f = 0$. Equation (17) is recovered for fully developed turbulent flow. The linear dependence of $f(R)$ with R in the transition region was found to describe the data adequately.

The Reynolds-number dependence of the shear stress is different for the three regimes. In laminar flow, the results of Von Karman [39] yield

$$\frac{\beta}{\Omega} = aR \quad (24)$$

Such theoretically well established results are not available for the shear stress in fully developed turbulent flow. However, Von Karman's [39] semi-empirical expression is available from a momentum balance using the $\frac{1}{7}$ -power velocity profile form commonly used in turbulent pipe flow. The result of Von Karman's work is used in the form

$$\frac{\beta}{\Omega} = 8.55 \times 10^{-3} R^{1.6} \quad (25)$$

Torque measurements on rotating disks are reported by Schlichting [40] in the form of torque coefficients. The angular shear stress is available from these studies. Surprisingly, its radial counterpart has not been explicitly reported nor correlated. Von Karman's expression is

compatible with the torque measurements, the flux expression given in the appendix, and the results of mass-transfer correlations.

In the transition region, the shear stress is made continuous with the forms for laminar and fully developed turbulent flow. With the experimental results of rotating ring electrodes in mind, the Reynolds-number limits were set as 1.5×10^5 to 3.0×10^5 for the transition region shear stress. These limits are slightly different from those for $f(R)$. A graph of the shear stress is given in figure 1.

To fit the rotating-disk data for fully developed turbulent flow (equation [2]), the shear stress and K must be consistent with the experimental mass-transfer correlation. Equation (A-10), developed in the appendix, for $d(y^+) = 1$, expresses the Sherwood number in terms of K and β/Ω as

$$Sh_{loc} = 0.01092 R^{1.8} Sc^{1/3} = R \left(\frac{\beta}{\Omega} \right)^{1/2} \frac{(KSc)^{1/3}}{1.2092} . \quad (26)$$

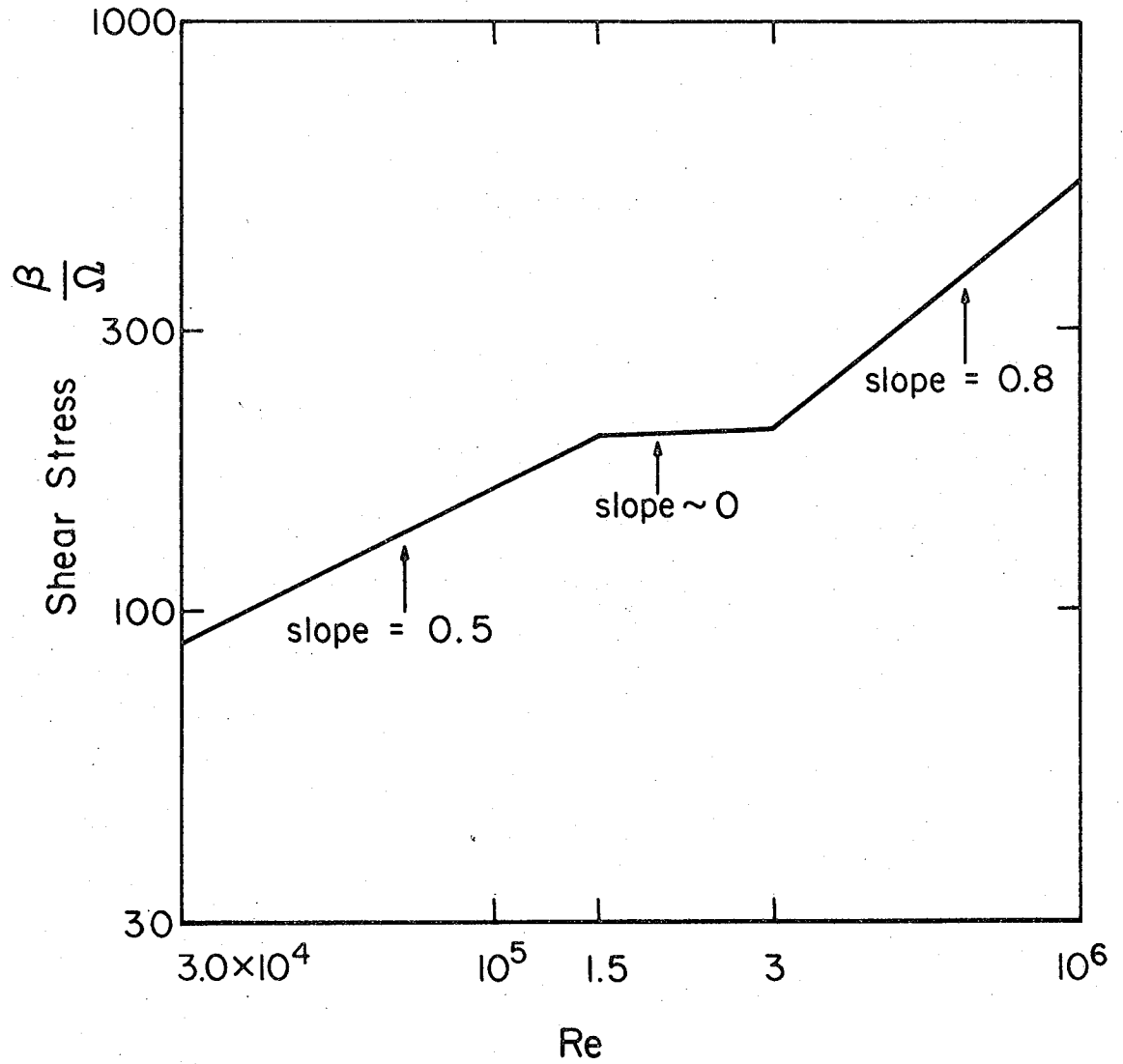
For β/Ω given by equation (25), $K = 2.9116 \times 10^{-3}$.

It is convenient and helpful to have the mass-transfer flow rate for extremely thin rings. Taking β/Ω as constant and the derivative as $1/\Gamma(4,3)$, equation (20) can be expanded and rearranged to yield

$$Sh_{loc} = \frac{1}{\Gamma(4/3)} \left(\frac{\beta}{3\Omega} \right)^{1/3} \frac{R^{5/3}}{(R^3 - R_i^3)} Sc^{1/3} \quad (27)$$

In particular, for laminar flow, this reduces to (see reference [11])

$$Sh_{loc,lam} = \frac{(a/3)^{1/3}}{\Gamma(4/3)} \frac{R^2 Sc^{1/3}}{(R^3 - R_i^3)^{1/3}} \quad (28)$$



XBL 805-9566A

Figure 1

The Reynolds number dependence of the radial shear stress.

Comparison of equation (27) with equation (28) shows the importance of the shear stress

$$\frac{Sh_{loc}}{Sh_{loc,lam}} = \left(\frac{\beta}{aR\Omega} \right)^{1/3} \quad (29)$$

To consider average mass-transfer rates, equation (27) is integrated for thin-ring conditions to give

$$\overline{Sh} = \frac{R \left(\frac{\beta}{\Omega} \right)^{1/3} Sc^{1/3}}{6 \Gamma(4/3)} \quad (30)$$

An analogous expression for laminar flow can be obtained so that the ratio of average Sherwood numbers is also given by equation (29) and is the ratio of the measured current to the current if laminar flow prevailed.

$$\frac{\overline{Sh}}{Sh_{lam}} = \left(\frac{\beta}{aR\Omega} \right)^{1/3} = \frac{I}{I_{lam}} \quad (31)$$

The last equality is important from a practical point since total currents are measured from limiting current experiments.

Experimental Data

Limiting currents were measured on thin rotating-ring electrodes. Rotation speeds were varied to investigate the laminar, transitional, and as much of the turbulent flow regime as possible. The electrochemical system used was the potassium ferricyanide - potassium ferrocyanide redox couple (approximately 0.005 molar) with an excess of potassium hydroxide (2 molar) as a supporting electrolyte. Ferricyanide was reduced at the nickel ring surface. Hydrogen evolution was suppressed by the relatively

large concentration of hydroxide. Thus broad, easily determined limiting-current plateaus were measured.

A 2.5 l cylindrical cell constructed from nickel with plastic end pieces served as the counterelectrode. The cell was jacketed. Water was circulated to control the electrolyte temperature at $25.00 \pm 0.05^\circ\text{C}$ as measured with a platinum resistance thermometer. A Princeton Applied Research potentiostat Model 371 with a PAR Model 175 function generator was used to control the reaction current. Polarograms were plotted on a Hewlett Packard Model 7044A x-y plotter. Electrode rotation speeds were measured with a calibrated "Strobotac" stroboscopic tachometer.

Three electrode assemblies were fabricated from nickel. All electrodes shared a common inner radius, r_i , of 3.163 ± 0.003 cm. The outer radius, r_o , was varied. The electrodes were thin, having ratios of the inner radius to the outer radius, r_i/r_o , of 0.9925, 0.9779, and 0.9221. The inner insulating disk and the outer insulating annulus were cast from Shell 826 epoxy and machined. The electrode and insulating surfaces were polished metallographically. The finishing step was a 0.05 micron diamond paste which yielded a highly polished surface with no visible scratches. The electrode rotator was fabricated to minimize vibration and electrode runout. A 1/2 horsepower Minarek DC speed controlled motor was used to drive the electrodes. Data were taken over rotation speeds which varied from 10 to 66.7 Hz (600 RPM to 4000 RPM).

Results and Discussion

The results presented in the ensuing figures are for $d(y^+) = 1$, that is, $D^{(t)}/\nu = Ky^+{}^3$. Subsequent comments will be made concerning a

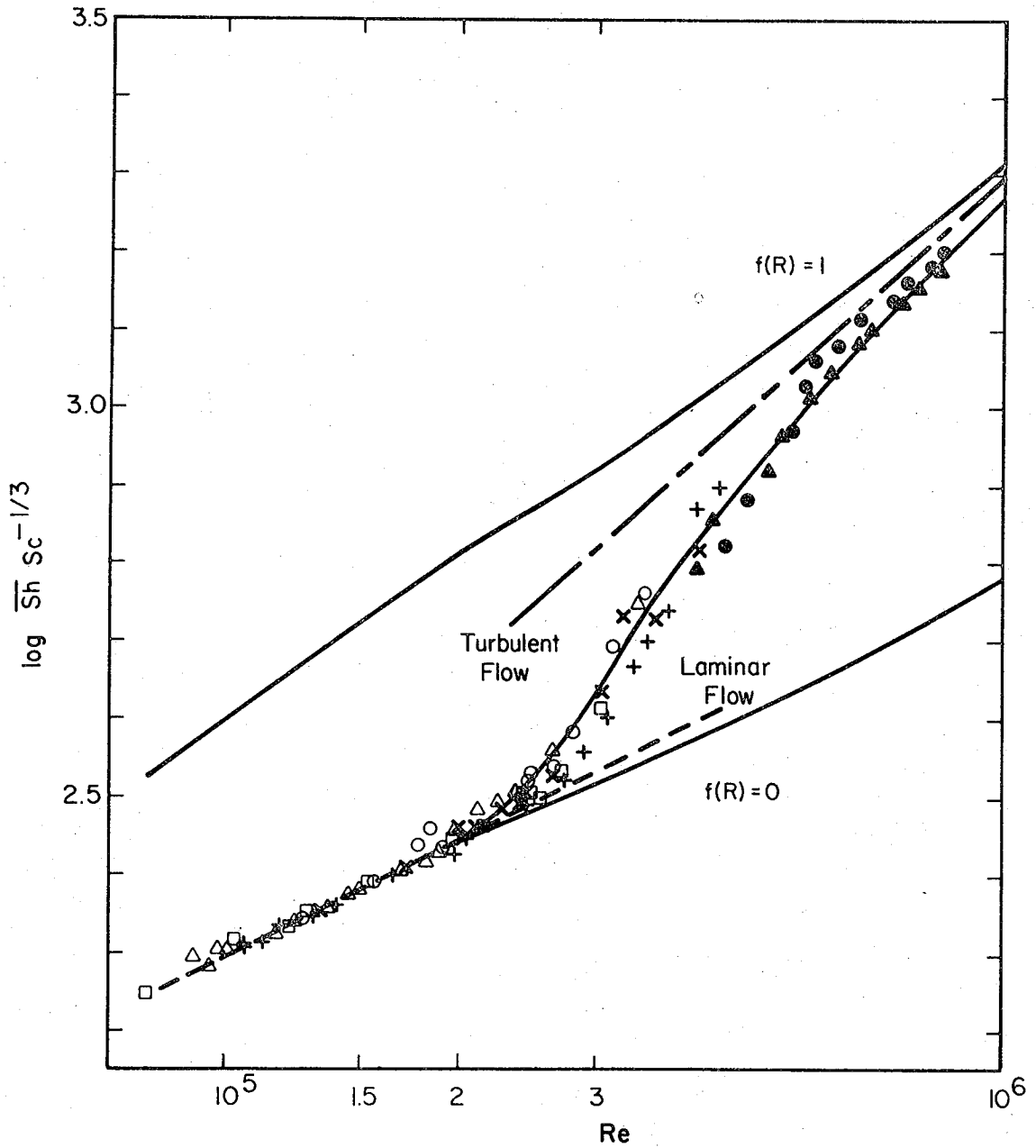
y^{+4} -dependence of $D^{(t)}/\nu$.

Figure 2 shows the results for average mass-transfer rates on a rotating disk compared to data given by Mohr and Newman [1] and Dagenet [8]. Agreement between the two is obtained over a considerable range of Reynolds numbers. The lines marked $f(R) = 0$ or $f(R) = 1$ are provided for reference. Note that absence of the eddy diffusivity term, $f = 0$, may result in an average flux below the corresponding laminar flow value.

In figure 3 the local value of the mass-transfer rate from the calculations is given. At a Reynolds number of 1.5×10^5 , the local Sherwood number drops below the laminar prediction due to the influence of the shear stress. However, at 2.0×10^5 the importance of turbulence in the transition region is seen as the eddy diffusivity term causes the local rate to increase. Finally, the full impact of turbulence exists at 3.0×10^5 and beyond.

The data from our experiments with rotating ring electrodes are given in figure 4. The current is made dimensionless with the current calculated as though laminar flow conditions existed. This normalization is particularly convenient for thin rings. Data are from the experiments described above. Agreement of the data with the calculations is adequate at low Reynolds numbers; however, at higher values the calculated results exceed the measurements. The rotating rings considered here are quite thin. Even so, the calculated current very rapidly approaches the rotating-disk result with increases in rotation speed. Somewhat surprisingly, the measured flux is below the laminar flow relationship, in transition and fully developed turbulent flow.

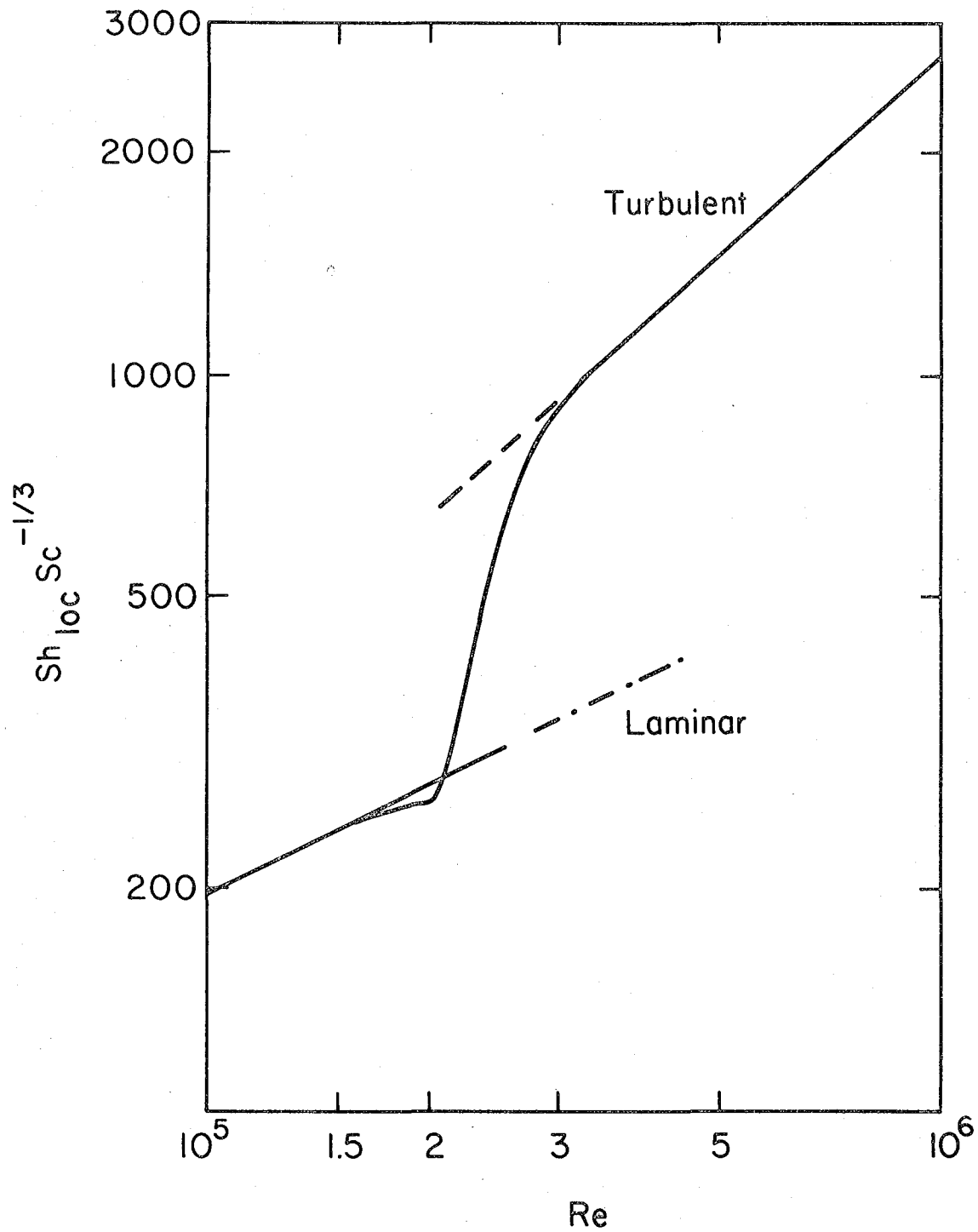
This fact led to our choice of von Karman's expression for the radial



XBL 805-9570A

Figure 2

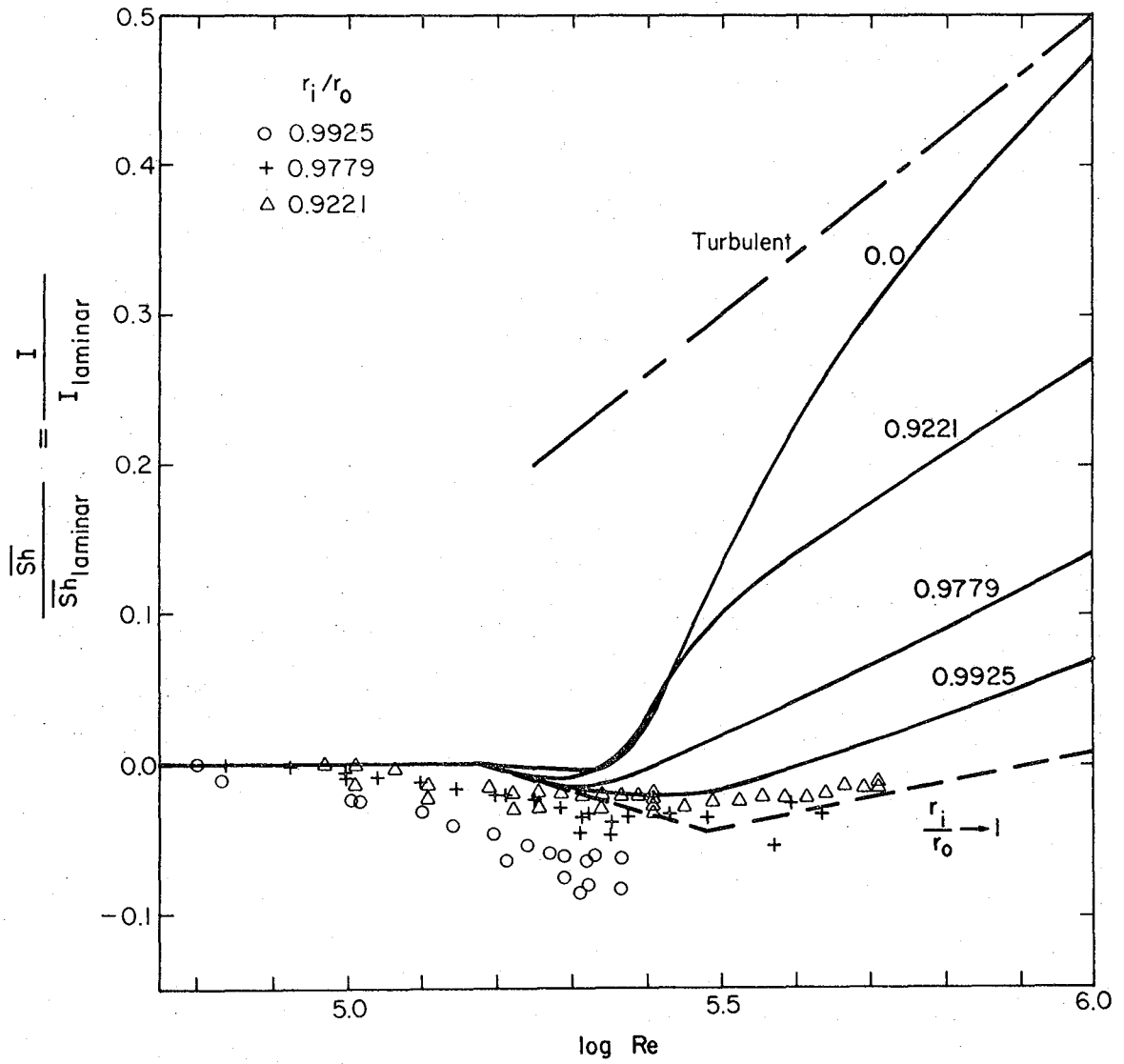
Overall mass-transfer rate vs Reynolds number for laminar, transition, and turbulent regimes. The Schmidt number for the data of Mohr and Newman \square 1192, Δ 1377, $+$ 1636, \circ 1760, \times 2465; for the data of Dagenet \bullet 1212, \blacktriangle 1980. The calculated results — are obtained from the solution of equation (22) with $K = 2.9 \times 10^{-3}$.



XBL 805-9567A

Figure 3

Local mass-transfer rate on a disk electrode vs Reynolds number.



XBL 805-9569A

Figure 4

The results of our mass-transfer experiments on rotating rings compared to the results of the calculations [equation (22) with $K = 2.9 \times 10^{-3}$].

shear stress, since it also lies below the laminar flow value for a certain range of Reynolds numbers, and it was anticipated that this could lead to a similar behavior for the mass-transfer rate in the thin-ring limit. On the other hand, expressions for the shear stress available from torque measurements always lie above laminar flow results and differ substantially from the measurements made on thin ring electrodes.

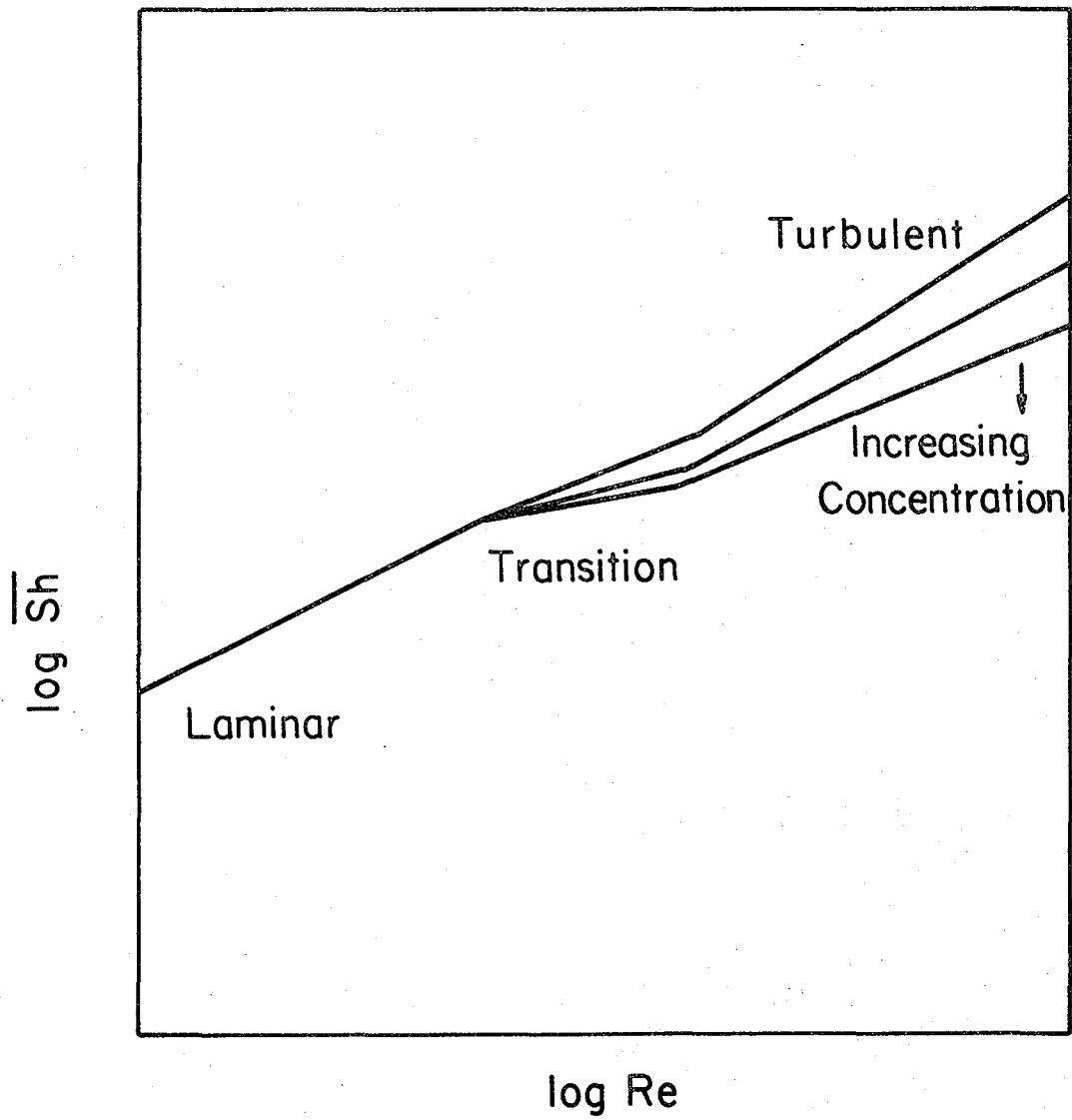
From the data presented in figure 4 and from the lines representing thin rings, it is clear that mass transfer in transition and turbulent flow can be less than that given by the laminar-flow expression. The results of the analysis show that the mass-transfer rate normalized with the laminar rate depends only upon the shear stress value.

Epelboin and his coworkers [41] have performed mass transfer experiments with thin rings in the presence of small amounts of drag-reducing compounds. Their results indicate qualitatively that small changes in the concentration of drag-reducing compounds cause a decrease in the mass-transfer rate, as well as the angular shear stress (torque), in transitional and turbulent flow. A representation of one of their graphs is given in figure 5.

Figure 6 is a comparison of the data taken by Delouis and Keddam [10] for a relatively thick ring, $r_1/r_0 = 0.6$. The comparison is good for all three regions.

Local mass-transfer rates representative of a number of different conditions are presented in figure 7.

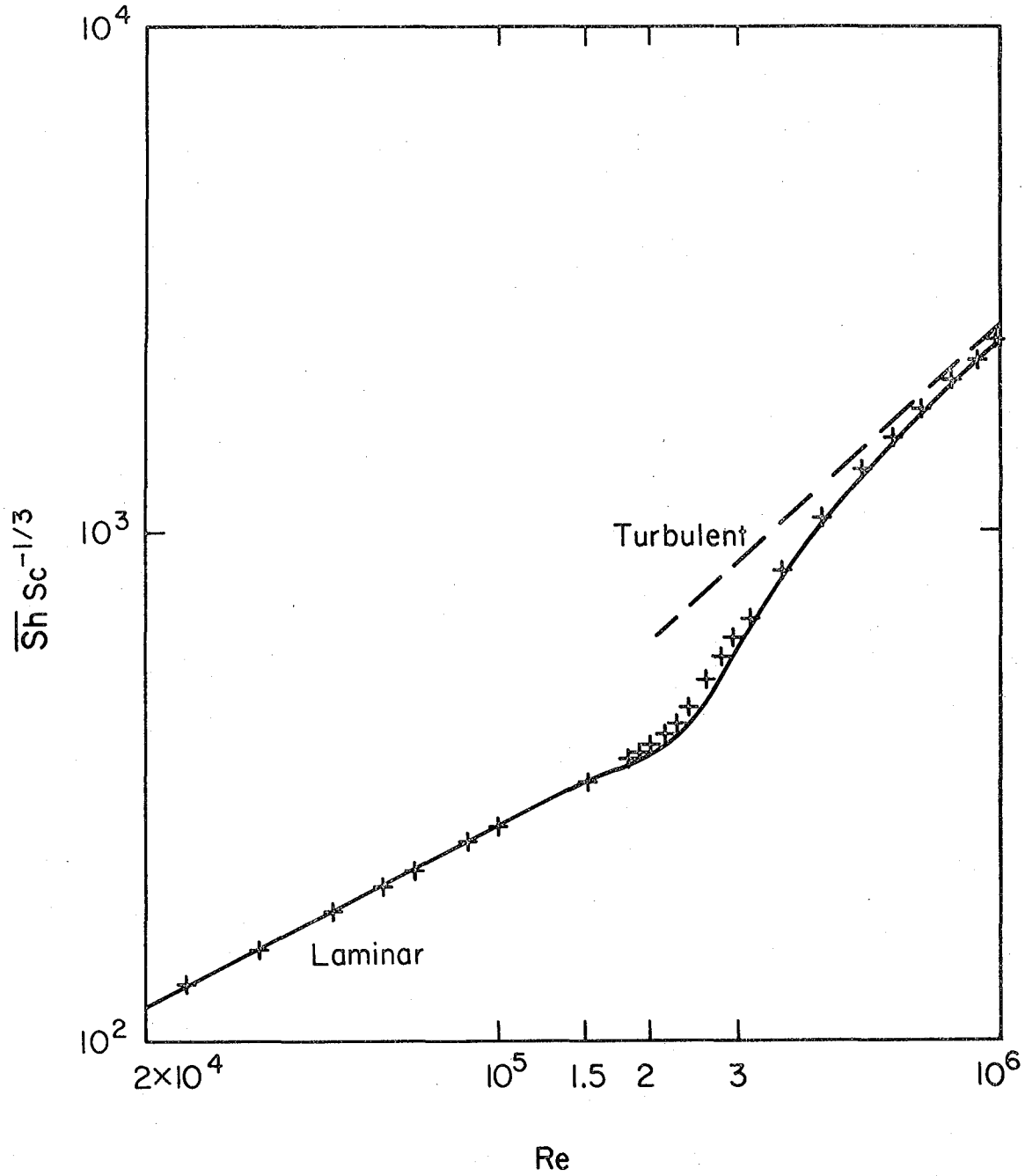
From the curves in figure 7, the local mass-transfer rate on rotating rings is high at the beginning of the mass-transfer region and approaches



XBL 807-10681

Figure 5

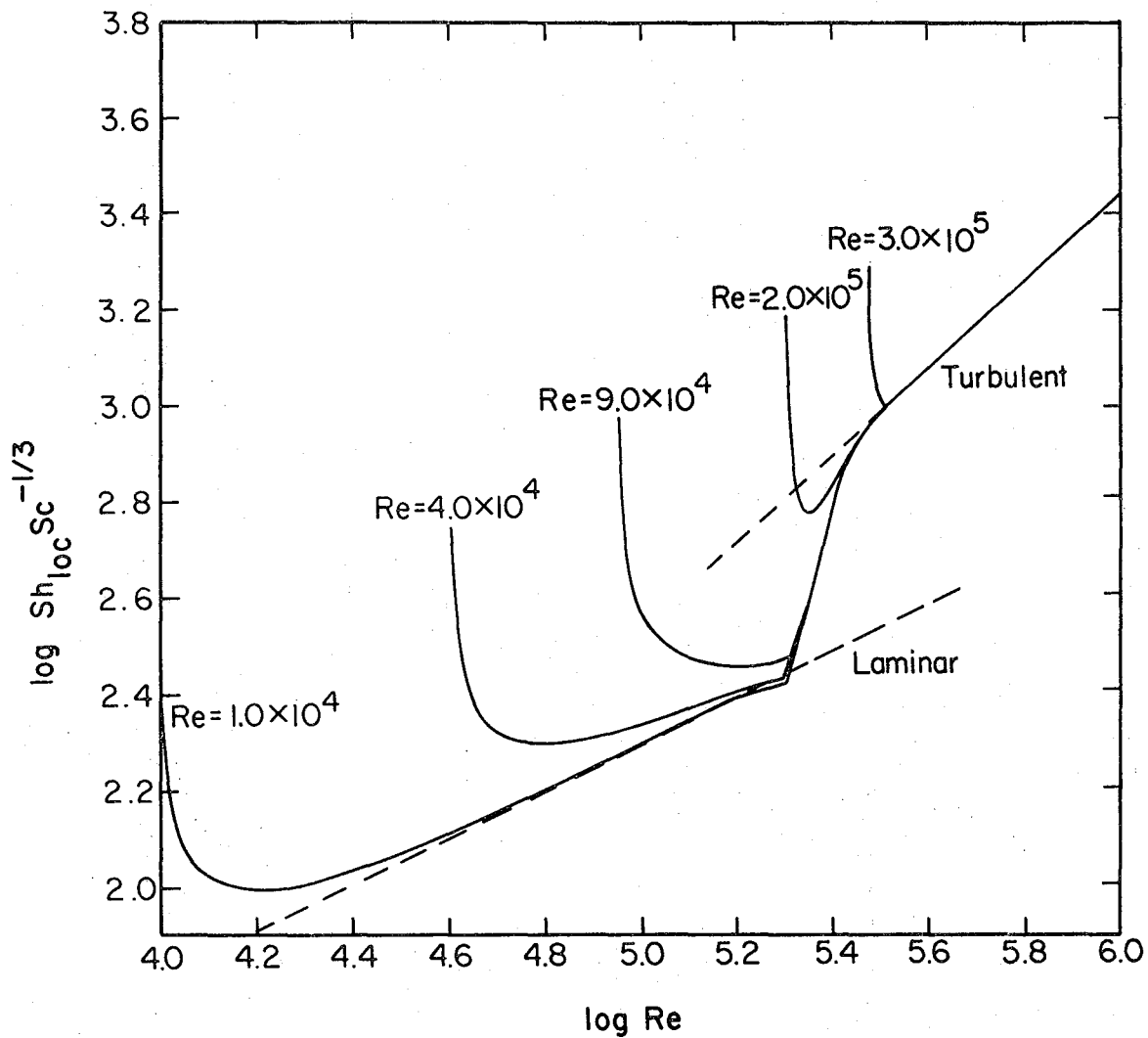
Qualitative illustration from reference 41 denoting the effect of increasing concentration of drag reducing agent on the mass-transfer rate for thin rotating rings.



XBL 805-9565A

Figure 6

Comparison of the mass-transfer data of Delouis and Keddam [10] on a rotating ring for dimensions $r_1/r_0 = 0.6$ with the results of the calculations [equation (22) with $K = 2.9 \times 10^{-3}$].



XBL 805-9568A

Figure 7

Local mass-transfer rate for rotating rings of various dimensions. The Reynolds number designation on the respective curves denotes the point at which mass transfer begins.

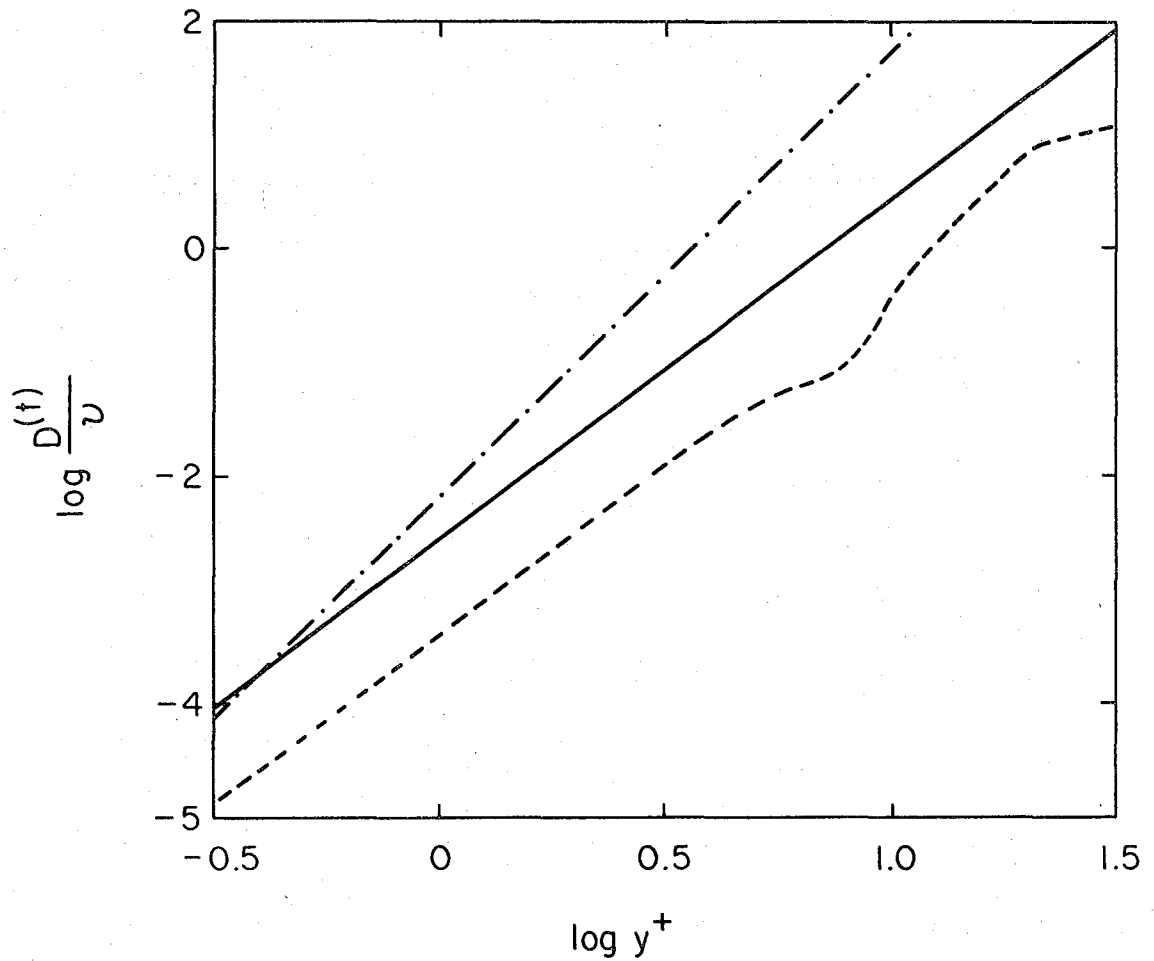
the rotating disk results downstream of the inner radius. This is true whether the diffusion boundary layer begins in laminar, transition, or fully developed turbulent flow. However, it is interesting to note that the sharp decline in the local Sherwood number observed near the inner edge of the ring is more pronounced in fully developed turbulent flow than in laminar flow. The mass-transfer entry length region in fully developed turbulent flow is shorter than in laminar flow. Newman [42] comments on this with regard to pipe flow.

It is worth mentioning that the discrepancy between measured and calculated values observed in figure 4 occurs in the development of the turbulent mass-transfer boundary layer. However, from figure 6 it is clear that the model does a good job of describing the average flux for thick rings, where the turbulent diffusion layer is more developed.

The results presented above are for $D^{(t)}/\nu = 2.9 \times 10^{-3} (y^+)^3$. In an attempt to obtain a better fit of the thin-ring data in transition and turbulent flow, $d(y^+)$ can be modified so that $D^{(t)}/\nu = Ky^+ (1 + K_1 y^+)$. With the value of K from Lin, Moulton, and Putnam [25], the disk results are fit reasonably well with the expression

$$\frac{D^{(t)}}{\nu} = 3.28 \times 10^{-4} y^{+3} (1 + 19.3y^+) . \quad (32)$$

In figure 8, $D^{(t)}/\nu$ is presented for these two forms in addition to the expression by Wasan, Tien, and Wilke [28]. The form by Wasan, Tien, and Wilke would fit the thin-ring data better than the two alternative forms, at the expense of a worse fit of the rotating-disk data in fully developed turbulent flow.



XBL 807-10682

Figure 8

Dependence of the eddy diffusivity upon the form used near the wall.
 $2.9 \times 10^{-3} y^{+3}$ — ; $3.3 \times 10^{-4} y^{+3} (1 + 19.3 y^+)$ - . - . ; form used by Wasan,
Tien, Wilke - - - - .

Only for very small values of y^+ is the y^{+3} , y^{+4} form smaller than the y^{+3} form ($y^+ \leq 0.41$). However, even with this more involved form, the thin-ring results in transition and turbulent flow are substantially the same. It is not possible to distinguish between these two forms from the data on rotating disks and rotating rings. Due to the simplicity of the governing equation with Ky^{+3} , this form is preferred.

Summary and Conclusions

A model is presented for the mass-transfer rate to rotating rings and rotating disks when laminar, transition, and turbulent flow exist upon different portions of the surface. The model compares well to rotating-disk data and to data for relatively thick rotating rings, existing in the literature. For the data given herein on thin rotating rings, the calculated results may exceed the measured mass-transfer rate in the transition and fully developed turbulent flow regimes. The contribution of the eddy diffusivity term to the overall mass transfer is too high, even for these thin rings. A y^{+3} form for the eddy diffusivity is used. However, no improvement in the comparison with the thin ring data was obtained for a y^{+3} , y^{+4} form.

Acknowledgment

This work was supported by the Division of Chemical Sciences, Office of Basic Energy Sciences, U.S. Department of Energy under Contract No. W-7405-Eng-48.

Appendix

Fully Developed Mass Transfer Rate in Fully Developed Flow

The intent is to obtain an expression for the local flux in fully developed turbulent flow (as R approaches infinity). The governing equation is given in the text as equation (6). For fully developed turbulent flow at high Schmidt numbers, it is appropriate to use a form for the velocity near the wall which is compatible with torque measurements made in fully developed turbulent flow and the results of Von Karman.

$$v_r = \frac{Qr^{1.6} \Omega^{1.8} y}{\nu^{0.8}} \quad (A-1)$$

and from the equation of continuity

$$v_y = - \frac{1.3Qr^{0.6} \Omega^{1.8} y^2}{\nu^{0.8}} \quad (A-2)$$

Substitution of these two expressions into equation (6) gives

$$\frac{Qr^{0.6} \Omega^{1.8} y}{\nu^{0.8}} \left[r \frac{\partial \theta}{\partial r} - 1.3y \frac{\partial \theta}{\partial y} \right] = \frac{\partial}{\partial y} \left[(D + D(t)) \frac{\partial \theta}{\partial y} \right] \quad (A-3)$$

A stretched variable can be defined as

$$Z = \frac{y^+ (KSc)^{1/3}}{g(R)} \quad (A-4)$$

which changes equation (A-4) to

$$\frac{g^3 Z}{\sqrt{QR}^{1.8}} \left[R \frac{\partial \theta}{\partial R} - R \frac{\partial \theta}{\partial Z} \frac{Z}{g} \frac{dg}{dR} - 1.3Z \frac{\partial \theta}{\partial Z} \right] = K \frac{\partial}{\partial Z} \left[(1 + g^3 Z^3) \frac{\partial \theta}{\partial Z} \right] \quad (A-5)$$

If g becomes small as R increases, $g^3 Z^3 \ll 1$. Then we can use the Lighthill similarity solution [compare equation (18)], which gives

$$g = \left[\frac{9K}{3.3} \frac{R^{3.3} - R_i^{3.3}}{R^{1.5}} \right]. \quad (\text{A-6})$$

This is contradictory because here g increases with R .

If g becomes large as R increases, $g^3 Z^3 \gg 1$ and g can be cancelled on the left and right sides of the equation. The left side is then negligible for large R , and the equation reduces to

$$\frac{\partial}{\partial Z} \left(Z^3 \frac{\partial \theta}{\partial Z} \right) = 0, \quad (\text{A-7})$$

which has no satisfactory solution near $Z = 0$.

Hence we are left with the conclusion that g must be constant as R increases, say $g = 1$. The left side is still negligible for large R , and the equation reduces to

$$\frac{\partial}{\partial Z} \left[(1 + Z^3) \frac{\partial \theta}{\partial Z} \right] = 0 \quad (\text{A-8})$$

The solution is

$$\theta = \frac{\int_0^Z \frac{dZ}{1+Z^3}}{\int_0^\infty \frac{dZ}{1+Z^3}} = \frac{\int_0^Z \frac{dZ}{1+Z^3}}{1.2092} \quad (\text{A-9})$$

This then yields

$$\begin{aligned} Sh_{loc} &= r \left. \frac{\partial \theta}{\partial y} \right|_{y=0} = r \left. \frac{\partial \theta}{\partial Z} \right|_{Z=0} \left(\frac{\partial Z}{\partial y} \right) \left(\frac{\partial y^+}{\partial y} \right) \\ &= \frac{r(KSc)^{1/3}}{1.2092\nu} \sqrt{\frac{\tau_o}{\rho}} = \frac{R(KSc)^{1/3}}{1.2092} \cdot \sqrt{\frac{\beta}{\Omega}}. \end{aligned} \quad (\text{A-10})$$

Equation (A-10) is a very useful relationship. Both the shear stress and the eddy diffusivity are involved in the expression for the transfer rate in fully developed mass transfer.

Notation

a	0.51023262
C_{∞}	bulk concentration, $\text{mol}\cdot\text{cm}^{-3}$
$d(y^+)$	function defined in equation (13)
D	diffusion coefficient, $\text{cm}^2\cdot\text{s}^{-1}$
$D^{(t)}$	eddy diffusivity, $\text{cm}^2\cdot\text{s}^{-1}$
$f(R)$	function defined in equation (23)
F	Faraday's constant, $96,487\text{ C}\cdot\text{mol}^{-1}$
g	function defined in equation (A-6)
i	local current density, $\text{A}\cdot\text{cm}^{-2}$
\bar{i}	average current density, $\text{A}\cdot\text{cm}^{-2}$
I	total current, A
K	constant defined in equation (11)
K_1	constant defined in equation (32)
n	the number of electrons transferred
Q	constant used in equation (A-1)
r	radial coordinate, cm
R	dimensionless radius, $r\sqrt{\Omega/\nu}$
Re	Reynolds number, $r^2\Omega/\nu$
Sc	Schmidt number, ν/D
Sh	Sherwood number, $ir/nFD C_{\infty}$

v_r	radial velocity, $\text{cm}\cdot\text{s}^{-1}$
v_y	axial velocity, $\text{cm}\cdot\text{s}^{-1}$
X	dimensionless variable defined in equation (15)
y	axial coordinate, cm
y^+	dimensionless axial position
Z	stretched boundary layer variable defined in equation (A-4)

Greek Symbols

$\beta(r)$	proportionality of v_r with y , s^{-1}
$\Gamma(4/3)$	0.89298, the gamma function of 4/3
θ	dimensionless concentration
μ	viscosity, $\text{g}\cdot\text{cm}^{-1}\cdot\text{s}^{-1}$
ν	kinematic viscosity of the solution, $\text{cm}^2\cdot\text{s}^{-1}$
ξ	Lighthill variable
ρ	solution density, kg cm^{-3}
τ_o	shear stress at the surface, $\text{g cm}^{-1} \text{s}^{-2}$
Ω	rotation speed, s^{-1}

Subscripts

i	inner radial position
o	outer radial position

References

1. Charles M. Mohr, Jr. and John Newman, "Mass Transfer to a Rotating Disk in Transition Flow," Journal of the Electrochemical Society, 123, 1687-1691 (1976).
2. N. Gregory, J. T. Stuart, and W. S. Walker, "On the Stability of Three-Dimensional Boundary Layers with Application to the Flow due to a Rotating Disk," Philosophical Transactions of the Royal Society of London, Mathematics and Physical Sciences, A 248, 155-199 (1956).
3. E. C. Cobb and O. A. Saunders, "Heat Transfer from a Rotating Disk," Proceedings of the Royal Society of London, A236, 343-351 (1956).
4. F. Kreith, J. H. Taylor, and J. P. Chong, "Heat and Mass Transfer from a Rotating Disk," Transactions of the American Society of Mechanical Engineers, Journal of Heat Transfer, 81, 95-105 (1959).
5. C. L. Tien and D. T. Campbell, "Heat and Mass Transfer from Rotating Cones," Journal of Fluid Mechanics, 17, 105-112 (1963).
6. B. T. Ellison and I. Coronet, "Mass Transfer to a Rotating Disk," Journal of the Electrochemical Society, 118, 68-72 (1971).
7. D. T. Chin and M. Litt, "An Electrochemical Study of Flow Instability on a Rotating Disk," Journal of Fluid Mechanics, 54, 613-625 (1972).
8. M. Daguinet, "Etude du Transport de Matiere en Solution a l'Aide des Electrodes a Disque et a Anneau Tournant," International Journal of Heat and Mass Transfer, 11, 1581-1596 (1968).
9. B. A. Kader and V. V. Dil'man, "Heat and Mass Transfer in an Inlet Section under Turbulent Flow Conditions and $Pr \gg 1$," Teoreticheskie Osnovy Khimicheskoi Tekhnologii, 7, 210-222 (1973).

10. C. Deslouis and M. Keddam, "Emploi d'Electrodes a Anneau Tournant a l'Etude du Transport de Matiere dans un Fluide en Regime Hydrodynamique Laminere ou Turbulent," International Journal of Heat and Mass Transfer, 16, 1763-1775 (1973).
11. B. Levich, Physiochemical Hydrodynamics, section 18, Prentice Hall, Inc., Englewood Cliffs, N. J. (1962).
12. J. Newman, "The Fundamental Principles of Current Distribution and Mass Transport in Electrochemical Cells," p. 294, Allen J. Bard, ed., Electroanalytical Chemistry, New York: Marcel Dekker, Inc., 1973, 6, 187-352.
13. W. Smyrl and J. Newman, "Limiting Current on a Rotating Disk with Radial Diffusion," Journal of the Electrochemical Society, 118, 1079-1081 (1971).
14. G. Cognet and M. Daguene, "Calcul du Flux Limite de Diffusion sur un Anneau Tournant," Academie des Sciences. Comptes Rendus. Serie C: Sci. Chimique, 270, 142-145 (1970).
15. T. S. Kornienko and M. Kh. Kishinevskii, "Diffusion Flow Towards Ring Electrodes on Rotating Disks," Elektrokhimiya, 8, 1759-1766 (1972).
16. D. B. Spalding, "Heat Transfer to a Turbulent Stream from a Surface with a Step-wise Discontinuity in Wall Temperature," International Developments in Heat Transfer, American Society of Mechanical Engineers, 1961, Part II. p. 439.
17. J. Kestin and L. N. Presen, "Application of Schmidt's Method to the Calculation of Spaldings' Function and of the Skin-Friction Coefficient in Turbulent Flow," International Journal of Heat and Mass

- Transfer, 5, 143-152 (1962).
18. J. Kestin and P. D. Richardson, "Heat Transfer Across Turbulent, Incompressible Boundary Layers," International Journal of Heat and Mass Transfer, 6, 147-189 (1963).
 19. L. F. Donovan, O. T. Hanna, and S. Yerazunis, "Similar Solutions of Turbulent Boundary Layer Heat and Mass Transfer Problems," Chemical Engineering Science, 22, 595-610 (1967).
 20. A. G. Smith and V. L. Shah, "The Calculation of Wall and Fluid Temperatures for the Incompressible Turbulent Boundary Layer, with Arbitrary Distribution of Wall Heat Flux," International Journal of Heat and Mass Transfer, 5, 1179-1189 (1962).
 21. G. O. Gardner and J. Kestin, "Calculation of the Spalding Function over a Range of Prandtl Numbers," International Journal of Heat and Mass Transfer, 6, 289-299 (1963).
 22. M. J. Lighthill, "Contribution to the Theory of Heat Transfer through a Laminar Boundary Layer," Proceedings of the Royal Society, A202, 359-377 (1950).
 23. E. V. Murphee, "Relation between Heat Transfer and Fluid Friction," Industrial and Engineering Chemistry, 24, 726-736 (1932).
 24. C. S. Lin, E. B. Denton, H. S. Gaskill, and G. L. Putnam, "Diffusion Controlled Electrode Reactions," Industrial and Engineering Chemistry, 43, 2136-2143 (1951).
 25. C. S. Lin, R. W. Moulton, and G. L. Putnam, "Mass Transfer between Solid Wall and Fluid Streams - Mechanism and Eddy Distribution Relationships in Turbulent Flow," Industrial and Engineering Chemistry, 45, 636-645 (1953).

26. H. Reichart, "Die Grundlagen des Turbulenten Warmenberanges," Archiv fur die Gesamte Warmetechnik, 6-7, 129-142 (1951). See also, N.A.C.A. Report TM 1408 (1957).
27. W. D. Rannie, "Heat Transfer in Turbulent Shear Flow," Journal of the Aeronautical Sciences, 23, 485-489 (1956).
28. D. T. Wasan, C. L. Tien, and C. R. Wilke, "Theoretical Correlation of Velocity and Eddy Viscosity for Flow Close to a Pipe Wall," Journal of the American Institute of Chemical Engineers, 9, 567-568 (1963).
29. W. Vielstich, "Der Zusammenhang Zwischen Nernsteschen Diffsionsschicht und Prandtlscher Strömungsgrenzschicht," Zeitschrift für Elektrochemie, 57, 646-655 (1953).
30. K. K. Sirkar and T. J. Hanratty, "Limiting Behavior of the Transverse Turbulent Velocity Fluctuations Close to a Wall," Industrial and Engineering Chemistry Fundamentals, 8, 189-192 (1969).
31. H. G. Elrod, Jr., "Note on the Turbulent Shear Stress near a Wall," Journal of the Aeronautical Sciences, 24, 468-469 (1957).
32. R. G. Deissler, "Analysis of Turbulent Heat Transfer, Mass Transfer, and Friction in Smooth Tubes at High Prandtl and Schmidt Numbers," N.A.C.A. Report 12 10 (1955).
33. J. S. Son and T. J. Hanratty, "Limiting Relation for the Eddy Diffusivity Close to a Wall," Journal of the American Institute of Chemical Engineers, 13, 689-696 (1967).
34. D. B. Spalding, "Contribution to the Theory of Heat Transfer across a Turbulent Boundary Layer," International Journal of Heat and Mass Transfer, 7, 743-761 (1964).

35. D. B. Spalding, "A Single Formula for the Law of the Wall," Journal of Applied Mechanics, Transactions American Society of Mechanical Engineers, Series E, 455-458 (1961).
36. B. Levich, "The Theory of Concentration Polarization," Acta Physico-chimica U.R.S.S., 17, 257-307 (1942).
37. B. Levich, "Theory of Concentration Polarization. II," Acta Physico-chimica U.R.S.S., 19, 117-132 (1944).
38. M. A. Leveque, "Les Lois de la Transmission de Chaleur par Convection," Annales des Mines, Memoires, 12-13, 201-299, 305-362, 381-415 (1928).
39. T. V. Karman, "Über Laminaire und Turbulente Reibung," Zeitschrift für Angewante Mathematik und Mechanik, 1, 233-252 (1921).
40. H. Schlichting, Boundary Layer Theory, McGraw-Hill, Inc., New York, N.Y. (1979).
41. C. Deslouis, I. Epelboin, B. Tribollet, L. Viet, "Local Mass Transfer in Turbulent Flow by Electrochemical Methods," Proceedings of the Fourth Biennial Symposium on Turbulence of Liquids, Science Press: Princeton, N.J., 254-265 (1975).
42. J. Newman, Electrochemical Systems, p. 320, Prentice-Hall, Inc., Englewood Cliffs, N.J. (1973).

List of Figure Captions

Figure 1

The Reynolds number dependence of the radial shear stress.

Figure 2

Overall mass-transfer rate vs Reynolds number for laminar, transition, and turbulent regimes. The Schmidt number for the data of Mohr and Newman \square 1192, Δ 1377, + 1636, \circ 1760, \times 2465; for the data of Daguinet \bullet 1212, \blacktriangle 1980. The calculated results — are obtained from the solution of equation (22) with $K = 2.9 \times 10^{-3}$.

Figure 3

Local mass-transfer rate on a disk electrode vs Reynolds number.

Figure 4

The results of our mass transfer experiments on rotating rings compared to the results of the calculations [equation (22) with $K = 2.9 \times 10^{-3}$].

Figure 5

Qualitative illustration from reference 41 denoting the effect of increasing concentration of drag reducing agent on the mass transfer rate for thin rotating rings.

Figure 6

Comparison of the mass-transfer data of Delouis and Keddam [10] on a rotating ring for dimensions $r_i/r_o = 0.6$ with the results of the calculations [equation (22) with $K = 2.9 \times 10^{-3}$].

Figure 7

Local mass-transfer rate for rotating rings of various dimensions. The Reynolds number designation on the respective curves denotes the point at which mass transfer begins.

Figure 8

Dependence of the eddy diffusivity upon the form used near the wall.

$2.9 \times 10^{-3} y^+{}^3$ ——— ; $3.3 \times 10^{-4} y^+{}^3 (1 + 19.3 y^+)$ - - - - ; form used by Wasan,

Tien, Wilke - - - - .

This report was done with support from the United States Energy Research and Development Administration. Any conclusions or opinions expressed in this report represent solely those of the author(s) and not necessarily those of The Regents of the University of California, the Lawrence Berkeley Laboratory or the United States Energy Research and Development Administration.